An Efficient Method for Nonlinear Distortion Calculation of the AM and PM Noise Spectra of FMCW Radar Transmitters

Alban Laloue, Jean-Christophe Nallatamby, Michel Prigent, *Member, IEEE*, Marc Camiade, and Juan Obregon, *Senior Member, IEEE*

***Abstract*—The demand for autonomous cruise control and collision warning/avoidance systems has increased in recent years. Many systems based on frequency-modulated continuous-wave (FMCW) radar have emerged and are still in development. Due to the high complexity of such systems, the accurate evaluation of the noise spectra in the transmitter chain driven by complex modulated signals is today a severe drawback due to the limitation of simulation tools. In this paper, a method is proposed to compute easily with any commercially available nonlinear simulator, the amplitude and phase modulated signal distortion introduced by the nonlinearities of the transmitter on an FMCW signal. First, the amplitude modulation (AM) and phase modulation (PM) noise spectra of the driving FMCW signal is derived from the knowledge of the continuous wave (CW) AM and PM noise spectra of the voltage-controlled oscillator (VCO), and the modulating saw-tooth signal applied. Using the narrow band envelope concept and a first-order expansion of the nonlinear transfer function of the transmitter, the transfer of the AM and PM noise spectra of the driving FMCW signal through the nonlinear transmitter chain and the resulting output distortion are then computed. This novel approach allows to compute with reduced computation time and very good accuracy the AM/AM, AM/PM, PM/PM, and PM/AM conversion terms in any nonlinear system driven by CW or FMCW signals. This new method has been applied to the characterization of a whole car radar transmitter operating at 77 GHz driven by an FMCW signal issuing from a VCO.**

A successful comparison between measured and simulated PM-to-AM conversion coefficients of this transmitter is shown, validating the proposed method.

***Index Terms*—Amplitude modulation (AM) and phase modulation (PM) noise spectra distortion simulation, frequency-modulated continuous-wave (FMCW) signal, narrow-band envelope, nonlinear transfer function.**

I. Introduction

THE demand for autonomous cruise control and collision warning/avoidance systems has increased in recent years. Many systems based on frequency-modulated continuous-wave (FMCW) radar are in development around the world [1]–[3]. For the car radar systems, the frequency source is a key building block. Its performance directly affects those of the millimeter-wave front-end and, consequently, those of the whole system. The linearity, phase, and amplitude noise spectra of the whole source directly affect the S/N ratio of the FMCW radar and, therefore, its range and its target discrimination capability. Due to the high complexity of such systems, the accurate evaluation of the noise spectra in the presence of complex modulated signals is today a severe drawback due to the limitation of system simulation tools, mainly large simulation time and consumption memory.

In order to evaluate the noise characteristics of the system, dedicated simulation tools and techniques are needed.

Today, commercial software is available to compute the noise spectra at circuit level. Unfortunately, in spite of recent implementation of efficient tools such as modified nodal analysis and numerical resolution by Krylov subspace algorithms [4], the noise calculation at system level requires large CPU time and is memory consuming. At present, the usual solution for designers to evaluate the amplitude modulation (AM)/phase modulation (PM) noise spectra of radar transmitter output signal is to simulate, firstly, the noise spectra of the voltage-controlled oscillator (VCO) and dielectric resonator oscillator (DRO), using the harmonic-balance and related techniques; namely, the conversion matrices [4]. The transformation of these noise spectra leading to equivalent noise generators at the input access of the transmitter is then needed. Finally, another noise analysis simulation allows to compute the output AM and PM noise spectra.

However, this simulation procedure with data treatment take approximately 40 mn for the transmitter shown in this paper.

In this paper, which is an extended version of [5], we propose a faster method to compute with any commercially available nonlinear simulator[1] the AM/AM, AM/PM, PM/PM, and PM/AM conversion terms introduced by the transmitter chain on the input noise spectrum: only 2 mn are necessary (to be compared to the previous 40 mn for the same transmitter) including simulation and data treatment times.

In Section I, the spectrum equation of a noisy FMCW signal is presented. Section II deals with a method for the computation of the AM and PM noise spectra distortion introduced by a

Manuscript received December 13, 2002; revised March 3, 2003. This work was supported under the European Community Program Esprit 38311 LOCOMOTIVE.

A. Laloue was with the Institut de Recherche en Communications Optiques et Microondes, Universite de Limoges, 19100 Brive, France. He is now with the AMP-C3C, 91944 Les Ulis, France (e-mail: laloue@amp-c3c.com).

J.-C. Nallatamby, M. Prigent, and J. Obregon are with the Institut de Recherche en Communications Optiques et Microondes, Department of Génie Electrique et Informatique Industrielle, Universite de Limoges, 19100 Brive, France (e-mail: jcn@brive.unilim.fr; prigent@brive.unilim.fr).

M. Camiade is with United Monolithic Semiconductors, 91401 Orsay, France (e-mail: camiade@ums-gaas.com).

Digital Object Identifier 10.1109/TMTT.2003.815271

[1]As a nonexhaustive list of computer-aided design (CAD) software, we can give *ADS* from Agilent Technologies, *Designer* from the Ansoft Corporation, *ELDORF* from Mentor Graphics, *Microwave Office* from AWR, *SPECTRERF* from Cadence, . . ., etc.

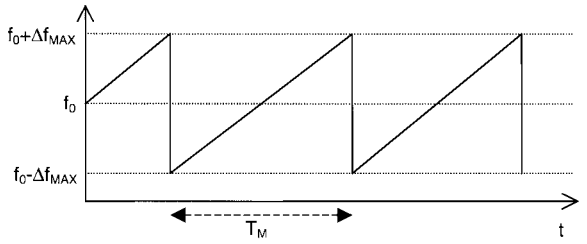

Fig. 1. Instantaneous frequency of an FMCW signal at the VCO output.

nonlinear transmitter on its input FMCW signal. The whole car radar source including the oscillator and transmitter chain is presented in Section III. In Section IV, the continuous wave (CW) phase and amplitude noise spectra at the output of this system source are computed with the previous method and compared with the measured ones. First, the AM and PM noise spectra of the driving FMCW signal are derived from the knowledge of the CW AM and PM noise spectra of the VCO, and the modulating saw-tooth signal applied. Using the narrow-band envelope concept and a first-order expansion of the nonlinear transfer function of the transmitter, the transfer of the AM and PM noise spectra of the driving FMCW signal through the nonlinear transmitter chain and the resulting output distortion are then computed.

II. FMCW Signal Spectrum

Radar for cruise control or collision warning/avoidance systems mostly rely on an FMCW signal, which is delivered by a VCO. The modulating signal is applied at the VCO control port in the way that the instantaneous output frequency of the VCO versus time will have the following shape, as illustrated in Fig. 1.

The frequency of the modulating saw-tooth is $\mathrm{F_M}$ and its period $\mathrm{T_M}$. The frequency-modulated carrier covers a bandwidth $2\Delta\mathrm{f_{max}}$ around the center frequency $\mathrm{f_0}$.

Before calculating the FMCW spectrum of this signal, let us be reminded of some definitions [6].

A. Envelope of Narrow-Band Signals

Let us define $a(t)$, as an AM and PM modulated signal written as

$$a(t) = A(t)\cos\left(\omega_o t + \Phi(t)\right) = \Re\left(A_+(t)\right) = \Re\left(\widetilde{A}(t)e^{j\omega_o t}\right) \tag{1}$$

where

- $A(t)$ and $\Phi(t)$ — time-varying amplitude and phase of the real signal $a(t)$, respectively;
- $\widetilde{A}(t)$ — $= A(t)e^{j\Phi(t)}$ complex envelope signal;
- ω_o — carrier frequency;
- $A_+(t)$ — $= A(t)e^{j\Phi(t)}e^{j\omega_0 t} = \widetilde{A}(t)e^{j\omega_0 t}$ named the analytic signal (or pre-envelope) of $a(t)$.

A complex envelope $\widetilde{A}(t)$ is said to be a slowly time-varying function if

$$\widetilde{A}(t) \approx \widetilde{A}(t + T_o) \tag{2}$$

where $T_o = 2\pi/\omega_o$ is the carrier period. This assumption can be written as

$$\frac{1}{A(t)}\frac{dA(t)}{dt} \ll \omega_o \text{ and } \frac{d\Phi(t)}{dt} \ll \omega_o \tag{3}$$

where (2) and (3) define narrow-band-limited signals.

In the frequency domain, we have the relations

$$A_+(f) = FT\left[A_+(t)\right] = \widetilde{A}(f - f_0) \tag{4}$$

$$A+(f) = \begin{cases} 2A(f), & \text{if } f > 0 \\ A(0), & \text{if } f = 0 \\ 0, & \text{if } f < 0 \end{cases} \tag{5}$$

$$A(f) = \frac{1}{2}\left[\widetilde{A}(f - f_0) + \widetilde{A}(-f + f_0)\right] \tag{6}$$

where $\widetilde{A}(f) = FT\lfloor\widetilde{A}(t)\rfloor$ and $A(f) = FT[A(t)]$.

B. Noiseless FMCW Signal Spectrum

An FMCW signal is defined in the time domain by (see Appendix I)

$$v(t) = V_0 \cos\left(\omega_0 t + \left[\frac{kt^2}{2}\right]_{T_M}\right) \tag{7}$$

where $[(kt^2)/2]_{T_M}$ indicates the saw-tooth equation on one period $\mathrm{T_M}$ of the phase modulation.

A straightforward calculation (detailed in Appendix I) leads to the equation of the complex envelope of the noiseless FMCW signal

$$\widetilde{V}(t) \approx V_{0_{\mathrm{FMCW}}} \sum_{n=\frac{-\Delta f_{\mathrm{MAX}}}{F_M}}^{n=\frac{\Delta f_{\mathrm{MAX}}}{F_M}} e^{j[n\omega_M t + \varphi_n]} \tag{8}$$

where $V_{0_{\mathrm{FMCW}}} = (V_0/\sqrt{2})\sqrt{F_M/\Delta f_{\mathrm{MAX}}}$ and $\varphi_n = (\pi/4) - n^2(\pi/2)(F_M/\Delta f_{\mathrm{MAX}})$, V_0 is the VCO output signal peak magnitude at the center carrier frequency ω_0 in CW mode (i.e., without modulation signal). The discrete spectrum of $v(t)$ is plotted in Fig. 2, with $\mathrm{T_M} = 2.5$ kHz and $\Delta\mathrm{f_{MAX}} = 100$ MHz.

The total number of spectral components is

$$N = \frac{2\Delta f_{\mathrm{MAX}}}{F_M} + 1. \tag{9}$$

In our case, there are 80 001 lines, spaced out from 2.5 kHz, in this spectrum. Note that the amplitude of the resulting deterministic signal spectrum remains constant in the frequency range between $\mathrm{f_0} - \Delta\mathrm{f_{max}}$ and $\mathrm{f_0} + \Delta\mathrm{f_{max}}$ [7].

C. Noisy FMCW Signal Spectrum

Let us now suppose that the deterministic modulated FMCW signal is noisy, i.e., it is modulated in amplitude and phase by the noise. It can be analytically shown (see detailed calculation in Appendix II) that, to the first order, the complex envelope

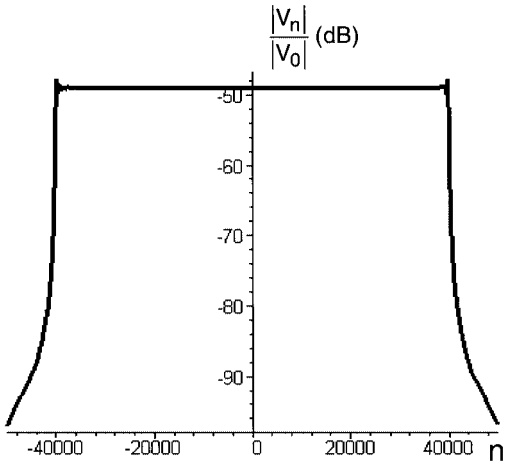

Fig. 2. Discrete spectrum of the complex envelop of the FMCW modulated signal.

expression of the FMCW signal, including its noise spectrum, can be written as

$$\widetilde{V}(t) \cong V_{0_{\mathrm{FMCW}}} \left\{ \sum_{n=-\frac{\Delta f_{\max}}{F_M}}^{n=\frac{\Delta f_{\max}}{F_M}} e^{j(n\omega_M t+\varphi_n)} \times \left(1+\frac{\Delta\widetilde{V}_0+j\cdot\Delta\widetilde{\phi}_0}{2}e^{j\Omega t} + \frac{\Delta\widetilde{V}_0^*+j\Delta\widetilde{\phi}_0^*}{2}e^{-j\Omega t} \right) \right\} \quad (10)$$

where $\Delta\widetilde{V}_0$ and $\Delta\widetilde{\phi}_0$ are, respectively, the first-order terms of the complex AM and PM noise modulations expansion series and Ω is the baseband frequency of the noise modulation. Equations (8) and (10) show that, at the first order, the resulting AM/PM spectrum of an FMCW signal is that of the CW signal shifted around each spectrum line.

III. Envelope Formalism for the Computation of AM and PM Noise Spectra Distortion Introduced by a Nonlinear Two-Port Circuit

In this section, the distortion introduced by linear and nonlinear two-port circuits on the AM/PM noise spectrum are calculated.

A. Linear Two-Port Circuit

1) General Formulation: Let us define a linear two-port circuit with a transfer function $\mathrm{H}(\omega)$ centered around ω_0. $\mathrm{v_{in}}(\mathrm{t})$ and $\mathrm{v_{out}}(\mathrm{t})$ are the real narrow-band-limited input and output signals (Fig. 3). $\mathrm{v_{in}}(\mathrm{t})$ and $\mathrm{v_{out}}(\mathrm{t})$ can be written as

$$v_{\mathrm{in}}(t)=\Re\left(\widetilde{V}_{\mathrm{in}}(t)e^{j\omega_o t}\right) \text{ and } v_{\mathrm{out}}(t)=\Re\left(\widetilde{V}_{\mathrm{out}}(t)e^{j\omega_o t}\right). \quad (11)$$

The Fourier transform of the input and output signals are related by

$$V_{\mathrm{out}}(\omega)=H(\omega)V_{\mathrm{in}}(\omega). \quad (12)$$

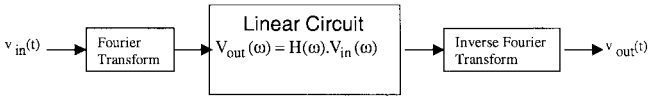

Fig. 3. Linear two-port circuit.

Now, using the Fourier transform of complex envelope signals (4)–(6), we obtain

$$\widetilde{V}_{\mathrm{out}}(\omega-\omega_0)=\frac{1}{2}\widetilde{H}(\omega-\omega_0)\widetilde{V}_{\mathrm{in}}(\omega-\omega_0). \quad (13)$$

Let us put $\Omega=\omega-\omega_0$, and by using (4), (13) becomes

$$\widetilde{V}_{\mathrm{out}}(\Omega)=\frac{1}{2}H_+(\omega_o+\Omega)\widetilde{V}_{\mathrm{in}}(\Omega). \quad (14)$$

As the spectrum of $\widetilde{V}_{\mathrm{in}}(\Omega)$ is confined around $\Omega=0$ (slowly time-varying modulation), the transfer function $H_+(\omega_o+\Omega)$ can be expanded in Taylor series around ω_{o} as

$$H_+(\omega_o+\Omega)=H_+(\omega_o)+\left.\frac{dH_+}{d\omega}\right|_{\omega_o}\Omega+\ldots. \quad (15)$$

Thus, from (14) and (15), and by using inverse Fourier transforms, we obtain

$$\begin{aligned}\widetilde{V}_{\mathrm{out}}(t)&=\frac{1}{2.\pi}\int_{-\infty}^{+\infty}\widetilde{V}_{\mathrm{out}}(\Omega)e^{j\Omega t}d\Omega\\&=\frac{1}{2}H_+(\omega_o)\frac{1}{2\pi}\int_{-\infty}^{+\infty}\widetilde{V}_{\mathrm{in}}(\Omega)e^{j\Omega t}d\Omega\\&\quad+\frac{1}{2}\left.\frac{dH_+}{d\omega}\right|_{\omega_o}\frac{1}{2\pi}\int_{-\infty}^{+\infty}\Omega\widetilde{V}_{\mathrm{in}}(\Omega)e^{j\Omega t}d\Omega+\ldots.\end{aligned} \quad (16)$$

By limiting the expansion to the first order, the output envelope signal can be written as

$$\widetilde{V}_{\mathrm{out}}(t)=\frac{1}{2}\left\{H_+(\omega_0)\widetilde{V}_{\mathrm{in}}(t)-j\left.\frac{dH_+}{d\omega}\right|_{\omega_o}\frac{d\widetilde{V}_{\mathrm{in}}(t)}{dt}\right\}. \quad (17)$$

This equation constitutes the basis of linear system analysis driven by modulated signals.

2) Application to FMCW Noisy Signals: Let us suppose that the input signal of the linear system under consideration is now an FMCW signal with its associated AM and PM noise spectra. The complex envelope of overall signal then can be written as

$$\widetilde{V}_{\mathrm{in}}(t)=\left(V_{o\_\mathrm{in}}+\delta V_{\mathrm{in}}(t)\right)e^{j(\Phi_{\mathrm{in}}(t)+\delta\phi_{\mathrm{in}}(t))} \quad (18)$$

where V_{o_in} and $\Phi_{\mathrm{in}}(t)$ are the deterministic amplitude and phase of the signal. $\delta V_{\mathrm{in}}(t)$ and $\delta\phi_{\mathrm{in}}(t)$ are, respectively, the AM and PM noise modulations with low modulation indexes.

Note that, in an FMCW signal, the amplitude is constant and the phase is time varying according to (8).

Let us reveal the magnitude and phase of the transfer function $H_+(\omega)$

$$H_+(\omega)=\hat{H}_+(\omega)e^{j\psi(\omega)}. \quad (19)$$

After some calculations (detailed in Appendix III), the relationship between the complex envelopes of input and output signals can be written as

$$\widetilde{V}_{\rm out}(t)=\frac{1}{2}H_{o+}\widetilde{V}_{\rm in}(t)\left\{1+\frac{1}{\hat{H}_{o+}}\frac{\partial\hat{H}_{+}}{\partial\omega}\bigg|_{\omega_0}\times\left(\frac{d\Phi_{\rm in}(t)}{dt}+\frac{d\delta\phi_{\rm in}(t)}{dt}-j\frac{1}{V_{o\_\rm in}}\frac{d\delta V_{\rm in}(t)}{dt}\right)\right\} \quad (20)$$

where $H_{0+}=H_{+}(\omega_0)$ and $\hat{H}_{0+}=\hat{H}_{+}(\omega_0)$.

In this expression, the first term $(1/2)H_{o+}\widetilde{V}_{\rm in}(t)$ represents the "ideal" output signal, which includes the linear term of the two-port circuit time delay.

This equation applies as well as to CW than FMCW signals with AM and PM noise spectra. Let us define the AM and PM noise spectra at a frequency offset Ω from the carrier, by revealing the AM and PM noise modulation indexes, respectively, $m_{a_{\rm in}}$ and $m_{\delta\phi_{\rm in}}$

$$\begin{aligned}\delta V_{\rm in}(t)&=m_{a_{\rm in}}V_{o\_\rm in}\cos(\Omega t+\varphi_a)=m_{a_{\rm in}}(t)V_{o\_\rm in}\\ \delta\phi_{\rm in}(t)&=m_{\delta\phi_{\rm in}}\cos(\Omega t+\varphi_\varphi)=m_{\delta\phi_{\rm in}}(t).\end{aligned} \quad (21)$$

From (19) and (20), the input signal envelope can be written as

$$\begin{aligned}\widetilde{V}_{\rm in}(t)&=V_{0\_\rm in}\left(1+m_{a_{\rm in}}(t)\right)e^{j\left(\Phi_{\rm in}(t)+m_{\delta\phi_{\rm in}}(t)\right)}\\ &\approx V_{0\_\rm in}\left(1+m_{a_{\rm in}}(t)+jm_{\delta\phi_{\rm in}}(t)\right)e^{j(\Phi_{\rm in}(t))}.\end{aligned} \quad (22)$$

$\widetilde{\rm V}_{\rm out}({\rm t})$ (20) then becomes

$$\widetilde{V}_{\rm out}(t)=\frac{1}{2}H_{o+}\widetilde{V}_{\rm in}(t)\left\{1+\frac{1}{\hat{H}_{o+}}\frac{\partial\hat{H}_{+}}{\partial\omega}\bigg|_{\omega_0}\times\left(\frac{d\Phi_{\rm in}(t)}{dt}+\frac{dm_{\delta\phi_{\rm in}}(t)}{dt}-j\frac{dm_{a_{\rm in}}(t)}{dt}\right)\right\}. \quad (23)$$

In the same way, we can write

$$\widetilde{V}_{\rm out}(t)=V_{0\_\rm out}\left(1+m_{a_{\rm out}}(t)+jm_{\delta\phi_{\rm out}}(t)\right)e^{j\Phi_{\rm out}(t)} \quad (24)$$

where $m_{a_{\rm out}}(t)$ and $m_{\delta\Phi_{\rm out}}(t)$, respectively, are the amplitude and phase noise modulation indexes of $\widetilde{V}_{\rm out}(t)$. By identifying the relation between the input and output noise terms of (23) and (24), it can be written

$$m_{a_{\rm out}}=m_{a_{\rm in}}(t)+\frac{1}{\hat{H}_{0+}}\frac{\partial\hat{H}_{+}}{\partial\omega}\bigg|_{\omega_0}\frac{dm_{\delta\phi_{\rm in}}(t)}{dt} \quad (25)$$

$$m_{\delta\Phi_{\rm out}}(t)=m_{\delta\Phi_{\rm in}}(t)-\frac{1}{\hat{H}_{0+}}\frac{\partial\hat{H}_{+}}{\partial\omega}\bigg|_{\omega_0}\frac{dm_{a_{\rm in}}(t)}{dt}. \quad (26)$$

By taking the Fourier transform of these two equations, the output amplitude and phase noise spectra defined as $S_{a\_\rm out}=\langle m^2_{a_{\rm out}}\rangle$ and $S_{\Phi\_\rm out}=\langle m^2_{\delta\phi_{\rm out}}\rangle$ can be expressed in function of the input amplitude and phase noise spectra $S_{a\_\rm in}=\langle m^2_{a_{\rm in}}\rangle$ and $S_{\Phi\_\rm in}=\langle m^2_{\delta\phi_{\rm in}}\rangle$

$$\begin{pmatrix}S_{a\_\rm out}(\Omega)\\ S_{\Phi\_\rm out}(\Omega)\end{pmatrix}=\begin{bmatrix}1 & \left(\frac{\Omega}{\hat{H}_{0+}}\frac{\partial\hat{H}_{+}}{\partial\omega}\bigg|_{\omega_0}\right)^2\\ \left(\frac{\Omega}{\hat{H}_{0+}}\frac{\partial\hat{H}_{+}}{\partial\omega}\bigg|_{\omega_0}\right)^2 & 1\end{bmatrix}\times\begin{pmatrix}S_{a\_\rm in}(\Omega)\\ S_{\Phi\_\rm in}(\Omega)\end{pmatrix}. \quad (27)$$

This matrix relates the input and output noise spectra in a linear system and can be easily computed from the knowledge of the transfer function of the circuit.

B. Nonlinear Two-Port Circuit

In this case, the two-port circuit transfer function $\rm H_{+}(\omega)$ becomes a nonlinear function of the input signal amplitude $\widetilde{\rm V}_{\rm in}$. The previous expression (14) must be now written as

$$\widetilde{V}_{\rm out}(\Omega)=\frac{1}{2}H_{+}\left(\omega_o+\Omega,\widetilde{V}_{\rm in}\right)\widetilde{V}_{\rm in}(\Omega). \quad (28)$$

By expanding this transfer function to the first order for a small AM index, the relationship between output and input signals can be obtained as

$$\widetilde{V}_{\rm out}(t)=\frac{1}{2}\left\{H_{+}(\omega_0)\widetilde{V}_{\rm in}(t)-j\frac{dH_{+}}{d\omega}\bigg|_{\omega_o}\frac{d\widetilde{V}_{\rm in}(t)}{dt}+\frac{\partial H_{+}}{\partial\widetilde{V}_{\rm in}}\bigg|_{\widetilde{V}_{\rm in}}\delta V_{\rm in}(t)\widetilde{V}_{\rm in}(t)\right\}. \quad (29)$$

By comparison with (20), a new term is added, corresponding to the nonlinear characteristic of the transfer function. Note that this equation can be considered as an extension of the calculation performed many years ago in order to calculate the noise spectrum using quasi-stationary approximations, in a one-port negative resistance oscillator [8]–[10].

With the same calculations as in annex 3, the relationship between $\widetilde{V}_{\rm out}(t)$ and $\widetilde{V}_{\rm in}(t)$ can be written as

$$\begin{aligned}\widetilde{V}_{\rm out}(t)=&\frac{1}{2}H_{o+}\widetilde{V}_{\rm in}(t)\\ &\times\left\{1+\frac{1}{\hat{H}_{o+}}\frac{\partial\hat{H}_{+}}{\partial\omega}\bigg|_{\omega_0}\times\left(\frac{d\delta\phi_{\rm in}(t)}{dt}+\frac{d\Phi_{\rm in}(t)}{dt}-j\frac{1}{V_{o\_\rm in}}\frac{d\delta V_{\rm in}(t)}{dt}\right)\right.\\ &+\left(\frac{1}{\hat{H}_{0+}}\frac{\partial\hat{H}_{+}}{\partial V_{o\_\rm in}}\bigg|_{V_{o\_\rm in}}+j\frac{\partial\Psi}{\partial V_{o\_\rm in}}\bigg|_{V_{o\_\rm in}}\right)\\ &\left.\times\delta V_{\rm in}(t)\right\}.\end{aligned} \quad (30)$$

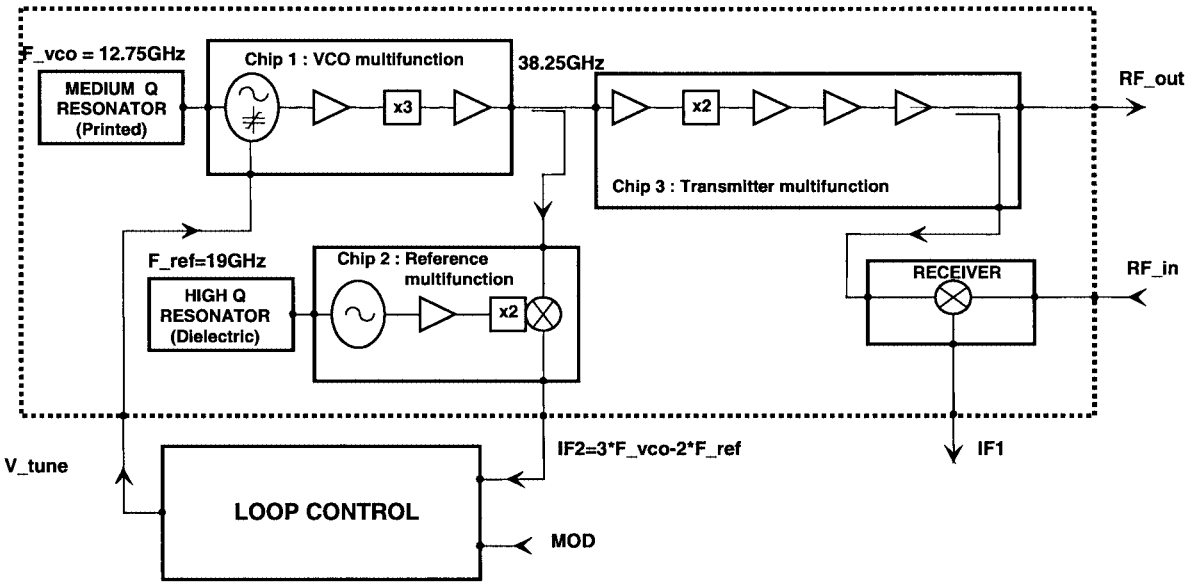

Fig. 4. Block diagram of a MMIC-based 77-GHz radar front-end.

The matrix equation relating the output AM and PM noise spectra to the input AM and PM noise spectra can be expressed as (31), shown at the bottom of this page.

The four coefficients of this matrix can be easily computed with one-tone harmonic-balance (HB) analysis of the two-port circuit under consideration by slightly varying the amplitude and frequency of the input generator.

Note that, in case of a frequency multiplier with rank N, (31) becomes (32), shown at bottom of this page, where $\widetilde{V}_{\rm out}$ is the output envelope signal associated to the output signal carrier at frequency $\mathrm{N}\omega_0$ and $\widetilde{\mathrm{V}}_{\rm in}$ is the input envelope signal associated to the input signal carrier at frequency ω_0. The nonlinear function of the frequency multiplier is expressed by

$$H_{N+} = \hat{H}_{N+} e^{j\psi_N} \tag{33}$$

with $\hat{H}_{N+} = V_{o\_\rm out}/V_{o\_\rm in}$.

These expressions are now applied to the calculation of the AM and PM noise spectra distortion introduced by the microwave chain of an FMCW car radar source. The monolithic microwave integrated circuits (MMICs) of this source have been designed and manufactured by United Monolithic Semiconductors (UMS), Orsay, France [1].

IV. Car Radar Millimeter-Wave Source

The manufactured front-end block diagram is shown in Fig. 4.

The technology based on a pseudomorphic high electron-mobility transistor (pHEMT) process with a quarter micrometer gate length (PH25) has been chosen for the source part up to 38-GHz frequency. The 77-GHz part was done on the 0.15-μm gate-length pHEMT process (PH15). Three main chips (numbered 1–3) are used for the millimeter-wave part of the source.

The VCO multifunction chip at 38 GHz is based on a sub-harmonic VCO at 12.75 GHz followed by a Q-band

$$\begin{pmatrix} S_{a\_\rm out}(\Omega) \\ S_{\Phi\_\rm out}(\Omega) \end{pmatrix} = \begin{bmatrix} \left(1+\dfrac{V_{o\_\rm in}}{\hat{H}_{0+}}\dfrac{\partial \hat{H}_+}{\partial V_{o\_\rm in}}\bigg|_{V_{o\_\rm in}}\right)^2 & \left(\dfrac{\Omega}{\hat{H}_{0+}}\dfrac{\partial \hat{H}_+}{\partial \omega}\bigg|_{\omega_0}\right)^2 \\ \left(V_{o\_\rm in}\dfrac{\partial \psi}{\partial V_{o\_\rm in}}\bigg|_{V_{o\_\rm in}}\right)^2 + \left(\dfrac{\Omega}{\hat{H}_{0+}}\dfrac{\partial \hat{H}_+}{\partial \omega}\bigg|_{\omega_0}\right)^2 & 1 \end{bmatrix} \times \begin{pmatrix} S_{a\_\rm in}(\Omega) \\ S_{\Phi\_\rm in}(\Omega) \end{pmatrix} \tag{31}$$

$$\begin{pmatrix} S_{a\_\rm out}(\Omega) \\ S_{\Phi\_\rm out}(\Omega) \end{pmatrix}_{N\omega_0} = \begin{bmatrix} \left(1+\dfrac{V_{o\_\rm in}}{\hat{H}_{N0+}}\dfrac{\partial \hat{H}_{N+}}{\partial V_{o\_\rm in}}\bigg|_{V_{0\_\rm in}}\right)^2 & \left(\dfrac{N\Omega}{\hat{H}_{N0+}}\dfrac{\partial \hat{H}_{N+}}{\partial \omega}\bigg|_{\omega_0}\right)^2 \\ \left(V_{o\_\rm in}\dfrac{\partial \psi_N}{\partial V_{o\_\rm in}}\bigg|_{V_{0\_\rm in}}\right)^2 + \left(\dfrac{\Omega}{\hat{H}_{N0+}}\dfrac{\partial \hat{H}_{N+}}{\partial \omega}\bigg|_{\omega_0}\right)^2 & N^2 \end{bmatrix} \times \begin{pmatrix} S_{a\_\rm in}(\Omega) \\ S_{\Phi\_\rm in}(\Omega) \end{pmatrix}_{\omega_0} \tag{32}$$

frequency tripler. The VCO is coupled to an external medium quality-factor resonator, which is made on a temperature —compensated soft substrate. This resonator is a transmittive filter connected to the MMIC thanks to two RF ports. This structure is the result of the best tradeoff between the following constraints: active device and varactor control, tuning range, out-of-band stability, and effect of inter-connections. The varactor is a pHEMT-based Schottky diode, the capacitor ratio is around three. The frequency tripler is built with an active transistor using its output current source nonlinearity. An output buffer amplifier at 38 GHz allows to reach the output power and contributes to the filtering.

The reference multifunction at 38 GHz is based on a high-performance oscillator at 19.25 GHz and on a second order sub-harmonic mixer. An external high-Q resonator gives the oscillator performance: good phase noise and frequency stability versus temperature and production spreads. This resonator is based on a high dielectric constant and a low-loss cylinder coupled to a microstrip line. The typical quality factor is around 24 000 at 10 GHz. The sub-harmonic mixer uses an unbiased transistor, the mixing nonlinearity is the variation of the drain-to-source conductance versus the gate-to-source voltage. The local oscillator (LO) signal is then applied to the gate, the RF signal is applied to the drain, and the IF output is extracted from the drain. An RF amplifier is also integrated, the main objective being to minimize the spurious leakage (undesirable mixing products) at the RF port.

The transmitter multifunction at 76 GHz integrates a doubler from 38 to 76 GHz and a medium power amplifier at 76 GHz. The input dynamic range of this chip is increased thanks to an input buffer amplifier at 38 GHz. This allows a lot of flexibility for coupling the VCO chip (filtering). As for the tripler of the VCO multifunction chip, the doubler uses an active transistor. A four-stage buffer amplifier at 77 GHz provides two outputs: one for the antenna and the other one for driving the LO of the receiver.

V. Phase and Amplitude Noise Spectra at the Source Output

A. Circuit Level Noise Spectra in CW Mode

1) AM/PM Noise Spectra of the VCO and DRO: Firstly, the amplitude and phase noise spectra at the outputs of the VCO (chip 1) and reference (chip 2) have been computed using the HB method and related techniques with a distributed noisy nonlinear model of a pHEMT [11]. Figs. 5 and 6 show the phase noise spectra of the VCO and DRO, respectively [12].

Note that the amplitude noise spectra measurement are not given because the noise floor of the measurement setup is very close to the measured spectrum. The measurements are inaccurate for frequency offset greater than 10 kHz. Note that, as will be shown later, the main contribution to the output AM noise spectrum results from the AM noise generated into the transmitter circuit itself.

2) AM/PM Noise Spectra Generated Into the Transmitter Circuit: Two types of uncorrelated noise spectra are present at the nonlinear two-port output. Firstly, the internal noise sources

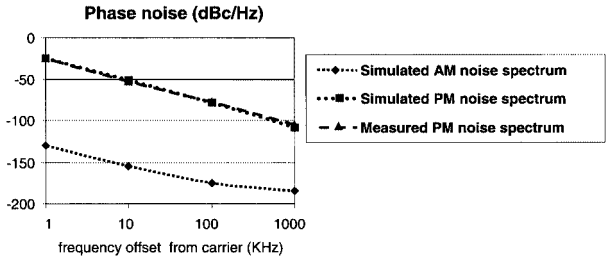

Fig. 5. VCO noise spectra (simulated and measured).

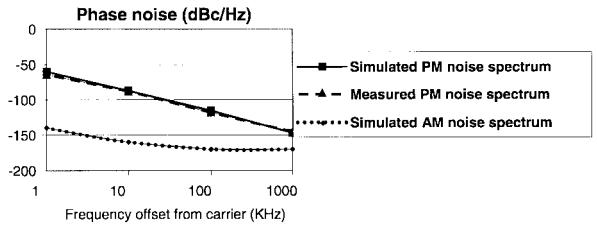

Fig. 6. Reference chip noise spectra (simulated and measured).

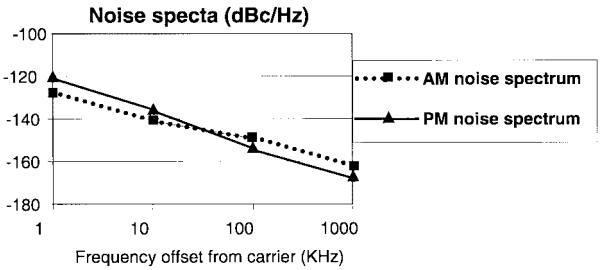

Fig. 7. AM and PM noise spectra of the transmitter due to internal low-frequency noise sources.

of the two-port circuit generate AM and PM noise spectra at its output.

As for the VCO and DRO, these noise spectra are computed with the HB method and related techniques. They are plotted in Fig. 7.

Secondly, a AM/PM distortion is generated in the nonlinear transmitter chain on the input AM and PM noise spectra issuing from the VCO. The formalism presented in Section II is dedicated to the computation of this distortion.

The four coefficients of the matrix (31) are computed from a one-tone HB simulation. They are shown in Fig. 8 versus output carrier frequency. A gain of 20 on simulation time is obtained with this method as compared with the classical noise analysis using the conversion matrices method associated with the HB analysis.

In order to verify the validity and accuracy of the proposed simulation method, two comparisons have been made.

Firstly, the PM/AM conversion through the transmitter chip has been measured for a modulation frequency of 300 kHz from the carrier. The measurement data are also plotted and compared with simulation results in Fig. 8(a).

Secondly, the AM/PM output noise spectrum of the whole radar source, including all the noise contributions, i.e., the distortion introduced by the transmitter chain and the noise generated in the transmitter itself, have been computed and compared to measured ones. These PM and AM noise spectra are

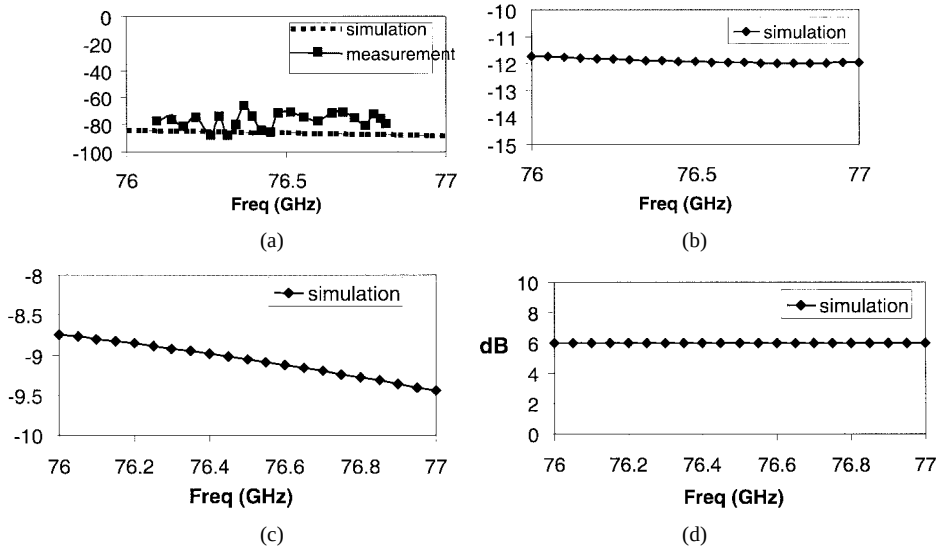

Fig. 8. Simulation of the conversion AM/AM, AM/PM, PM/AM, and PM/PM of a transmitter with $\Omega = 300$ kHz and measurement of PM-to-AM conversion.

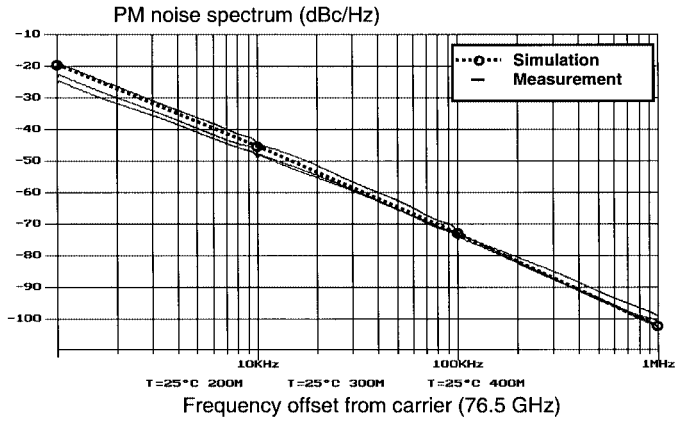

Fig. 9. Transmitter PM noise spectrum.

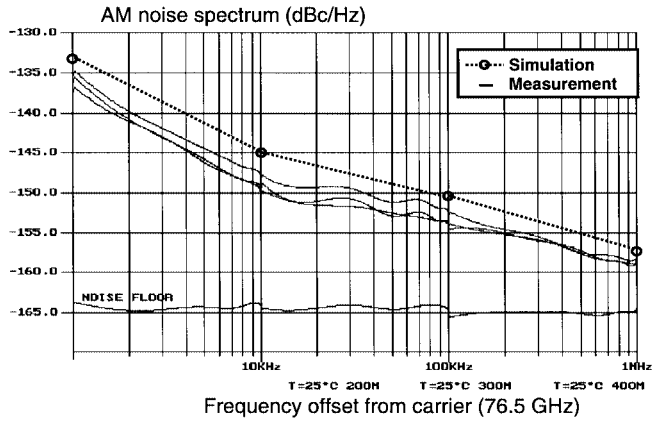

Fig. 10. Transmitter AM noise spectrum.

shown in Figs. 9 and 10 at frequencies around 76.5 GHz. For each noise characteristic, three input frequencies are considered: one corresponds to $\mathrm{IF2} = 200$ MHz, the second one is for $\mathrm{IF2} = 300$ MHz, and the last one is for $\mathrm{IF2} = 400$ MHz (see Fig. 4 for signification of IF2). Note that these spectra are very close whatever the input frequency. The simulation is done for a frequency corresponding to an $\mathrm{IF2} = 300$ MHz (center of the band).

A good agreement is obtained between these results, validating the proposed method, which enables a dramatic reduction in the computation time.

B. Noise Spectra With FMCW Signal

From the AM/PM noise spectrum computed in the CW mode, (10) easily allows to compute the noise spectra of the FMCW modulated signal. Let us recall that this spectrum is composed of a high number of lines centered around the carrier frequency (or average frequency) ω_0 and spaced from ω_{M}, which is the modulating frequency of the saw-tooth signal.

Each line of this signal is then modulated by the noise, as found in (10). To compute the resulting PM and AM phase noise spectra, we have computed these spectra around each line of the deterministic spectrum for offset frequencies from 30 Hz to 10 kHz. All the noise spectra contributions have then been added.

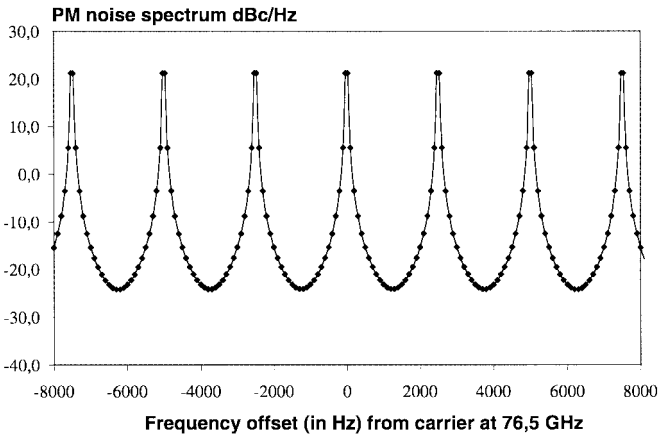

Fig. 11. PM noise spectrum of the FMCW signal.

The output noise spectra of the simulated chirp signal is shown in Fig. 11 and 12 for only seven spectral lines among the 80 001 lines.

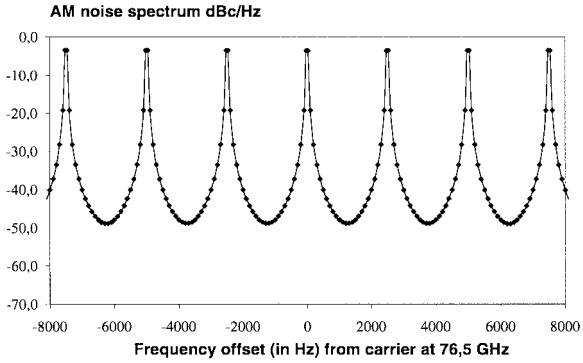

Fig. 12. AM noise spectrum of the FMCW signal.

It must be noted that the resulting noise level at the central frequency between two consecutive lines (spaced from 2.5 kHz) of the noiseless FMCW spectrum $\mathrm{f_0}+\mathrm{k}\,F_M$ and $\mathrm{f_0}+(\mathrm{k}+1)\,F_M$ is mainly due to the internal low-frequency noise sources of the VCO at $F_M/2$, which are up converted, and generate this central frequency as a result of correlated upper noise sideband of $\mathrm{f_0}+\mathrm{k}\,F_M$ and lower noise sideband of $\mathrm{f_0}+(\mathrm{k}+1)\,F_M$.

These AM and PM noise spectra give some information to designers on the target discrimination capability of the source. This specification is directly related to the ratio between the power carried by the deterministic discrete lines spectrum at frequencies 76.5 GHz $\pm$n 2.5 kHz (n = 1 to 80 001) and the noise between two consecutive lines of this spectrum. The PM noise spectrum influences on the discrimination between two targets of very different equivalent cross-sectional radar (a bicycle and truck), while the AM noise spectrum is more involved through the decoupling between emission and reception channels.

From these specifications, radar designers can choose the best architecture of the associated receiver, i.e., homodyne receiver, switching receiver or heterodyne receiver, in order to obtain the desired discrimination capability and noise figure of the whole automotive radar.

VI. Conclusion

A new method based on the envelope formalism has been proposed to simulate the noise spectra of a FMCW signal passing through a nonlinear system. This method allows to obtain efficiently and accurately the four conversion coefficients linking the AM and PM noise spectra at the input and output of the system. By applying this calculation together with the envelop formalism to the transmitter chip of an FMCW radar, the AM and PM noise output spectra have been computed. Comparisons with measurements have demonstrated a good accuracy.

The proposed calculation method can be used to optimize the conversion coefficients of the MMIC transmitter chain, and then to improve the sensitivity of the radar.

Appendix I

Calculation of the Chirp-Signal Spectrum

A chirp signal is the result of a frequency-modulated carrier by a saw-tooth signal, as shown in Fig. 1. The modulated signal can be written as

$$v(t) = V_0 \cos\left(\omega_0 t + \left[\frac{kt^2}{2}\right]_{T_M}\right) \tag{A1.1}$$

where $[(kt^2)/2]_{T_M}$ indicates the saw-tooth equation on one period $\mathrm{T_M}$ of the phase modulation. On one period, its complex envelope can be written as

$$\widetilde{V}(t) = V_0 e^{j((kt^2)/2)} \tag{A1.2}$$

where $k = 2((\Delta f_{\mathrm{MAX}})/T_M)$ is the slope of the saw-tooth signal. The period of the saw-tooth is $\mathrm{T_M}$. The modulated signal covers a bandwidth $2\Delta f_{\mathrm{MAX}}$ around the center frequency $\mathrm{f_0}$.

The signal spectrum and its complex envelope are related by

$$V(\omega) = FT\big(v(t)\big) = \frac{1}{2}\left[\widetilde{V}(\omega-\omega_0) + \widetilde{V}(-\omega-\omega_0)\right]. \tag{A1.3}$$

By calculating $\widetilde{V}(\omega)$, we can obtain the spectrum of $v(t)$. The complex envelope $\widetilde{V}(t)$ is periodic with period $\mathrm{T_M}$. It can then be expanded in Fourier series

$$\widetilde{\mathrm{V}}(t) = \sum_{-\infty}^{+\infty} \mathrm{V_n} e^{\mathrm{j n}\omega_{\mathrm{M}}\mathrm{t}} \tag{A1.4}$$

with

$$V_n = \frac{V_0}{T_M} \int_{\frac{-T_M}{2}}^{\frac{T_M}{2}} e^{j\left(((kt^2)/2) - n\omega_M t\right)} dt \tag{A1.5}$$

where $\omega_M = 2\pi F_M$ and $F_M = 1/T_M$.

This integral can be analytically calculated and $\mathrm{V_n}$ becomes

$$V_n = \frac{V_0}{2}\sqrt{\frac{F_M}{\Delta f_{\mathrm{MAX}}}} e^{-j((n^2\omega_M^2)/2k)}\big(e(-x_1) + e(x_2)\big) \tag{A1.6}$$

with $\mathrm{e(x)} = \mathrm{C(x)} + \mathrm{jS(x)}$, where $\mathrm{C(x)}$ and $\mathrm{S(x)}$ are Fresnel integrals with

$$x_1 = \sqrt{\frac{\Delta f_{\mathrm{MAX}}}{F_M}}\left[1 + n\frac{F_M}{\Delta f_{\mathrm{MAX}}}\right]$$
$$x_2 = \sqrt{\frac{\Delta f_{\mathrm{MAX}}}{F_M}}\left[1 - n\frac{F_M}{\Delta f_{\mathrm{MAX}}}\right]. \tag{A1.7}$$

As the ratio $((\Delta f_{\mathrm{MAX}})/F_M) \gg 1$, (A1.7) can then be calculated from the asymptotic behavior of the Fresnel integrals and the complex envelope of the signal $v(t)$ finally can be written as

$$\widetilde{V}(t) \approx V_{0_{\mathrm{FMCW}}} \sum_{n=\frac{-\Delta f_{\mathrm{MAX}}}{F_M}}^{n=\frac{\Delta f_{\mathrm{MAX}}}{F_M}} e^{j[n\omega_M t + \varphi_n]} \tag{A1.8}$$

where $V_{0_{\mathrm{FMCW}}} = (V_0/\sqrt{2})\sqrt{(F_M/\Delta f_{\mathrm{MAX}})}$ and $\varphi_n = (\pi/4) - n^2(\pi/2)(F_M/\Delta f_{\mathrm{MAX}})$

APPENDIX II

CALCULATION OF THE FMCW SIGNAL NOISE SPECTRUM

A. CW Noisy Signal

Firstly, let us remind the equation of a noisy CW signal. From (1), the expression of the complex envelope of a modulated signal with AM and PM noise modulations can be written as

$$\widetilde{V}(t) = \big(V_0 + \delta V(t)\big)e^{j(\Phi_0+\delta\phi(t))} \tag{A2.1}$$

where $\delta V(t)$ and $\delta\phi(t)$ can be written as pseudosinusoïdal equivalent modulations at a baseband modulating frequency Ω as follows:

$$\delta V(t) = \Delta V\cos(\Omega t + \varphi_a) \tag{A2.2}$$

$$\delta\phi(t) = \Delta\phi\cos(\Omega t + \varphi_p) \tag{A2.3}$$

with $\langle\delta v(t)^2\rangle = (1/2)\langle\Delta V^2\rangle$ and $\langle\delta\phi(t)^2\rangle = (1/2)\langle\Delta\phi^2\rangle$; $\varphi_{\rm a}$ and $\varphi_{\rm p}$ being random phases. By taking into account the low indexes of the noise modulations, we can write

$$\delta V(t) \ll V_0 \tag{A2.4}$$

$$\frac{d\delta\phi(t)}{dt} \ll \omega_0. \tag{A2.5}$$

A first-order development of (A2.1) using (A2.2) and (A2.3) gives

$$\widetilde{V}(t) \cong V_0 e^{j\Phi_0}\left(1 + \frac{\Delta\widetilde{V} + j\Delta\widetilde{\phi}}{2}e^{j\Omega t} + \frac{\Delta\widetilde{V}^* + j\Delta\widetilde{\phi}^*}{2}e^{-j\Omega t}\right) \tag{A2.6}$$

with

$$\Delta\widetilde{V} = \Delta V e^{j\varphi_a} \text{ and } \Delta\widetilde{\phi} = \Delta\phi e^{j\varphi_p}. \tag{A2.7}$$

The term $V_0e^{j\Phi_0}$ represents the complex envelope of the CW noiseless carrier signal.

B. FMCW Noisy Signal

The complex envelope of an FMCW noiseless signal can be written as (A1.8)

$$\widetilde{V}(t) \approx V_{0_{\rm FMCW}} \sum_{n=\frac{-\Delta f_{\rm MAX}}{F_M}}^{n=\frac{\Delta f_{\rm MAX}}{F_M}} e^{j[n\omega_M t+\varphi_n]} \tag{A2.8}$$

where $V_{0_{\rm FMCW}} = (V_0/\sqrt{2})\sqrt{(F_M/\Delta f_{\rm MAX})}$ and $\varphi_n = (\pi/4) - n^2(\pi/2)(F_M/\Delta f_{\rm MAX})$ In the presence of noise, this signal is also amplitude and phase modulated and can be written as (A2.6)

$$\widetilde{V}(t) \cong \big(V_{0_{\rm FMCW}} + \delta V(t)\big)\sum_{n=-\frac{\Delta f_{\max}}{F_M}}^{n=\frac{\Delta f_{\max}}{F_M}} e^{j(n\omega_M t+\varphi_n)}e^{j\delta\phi(t)}. \tag{A2.9}$$

On the other hand, theoretically, the AM and PM noise spectra are also modulated at the same rate $\omega_{\rm M}$. Thus, from (A2.2), (A2.3), and (A2.7), the amplitudes $\Delta\widetilde{\rm V}$ and $\Delta\widetilde{\Phi}$ at the baseband frequency Ω write as

$$\Delta\widetilde{V} = \sum_{p=-\infty}^{+\infty}\Delta\widetilde{V}_p e^{jp\omega_M t} \text{ and } \Delta\widetilde{\phi} = \sum_{p=-\infty}^{+\infty}\Delta\widetilde{\phi}_p e^{jp\omega_M t} \tag{A2.10}$$

and (A2.9) becomes

$$\begin{aligned}\widetilde{V}(t) \cong V_{0_{\rm FMCW}} &\cdot\left\{\sum_{n=-\frac{\Delta f_{\max}}{F_M}}^{n=\frac{\Delta f_{\max}}{F_M}} e^{j(n\omega_M t+\varphi_n)}\right.\\ &\times\left(1 + \frac{\Delta\widetilde{V}_0 + j\Delta\widetilde{\phi}_0}{2}e^{j\Omega t} + \frac{\Delta\widetilde{V}_0^* + j\Delta\widetilde{\phi}_0^*}{2}\right.\\ &\left.\times e^{-j\Omega t}\right) + \sum_{n=-\frac{\Delta f_{\max}}{F_M}}^{n=\frac{\Delta f_{\max}}{F_M}}\sum_{\substack{p=-\infty\\ p\neq 0}}^{+\infty}\frac{\Delta\widetilde{V}_p + j\Delta\widetilde{\phi}_p}{2}\\ &\times e^{j([(n+p)\omega_M+\Omega]t+\varphi_n)} + \frac{\Delta\widetilde{V}_p^* + j\Delta\widetilde{\phi}_p^*}{2}\\ &\left.\times e^{j([(n+p)\omega_M-\Omega]t+\varphi_n)}\right\}\end{aligned} \tag{A2.11}$$

For the sake of clarity, the first order of the resulting AM and PM noise amplitudes $\Delta\widetilde{V}_0$ and $\Delta\widetilde{\phi}_0$ have been isolated from higher order products. Practically, the noise may be considered as a constant in the function of the VCO tuning voltage, else it does not vary with the modulating signal. We can then neglect the coefficients $\Delta\widetilde{V}_p$ and $\Delta\widetilde{\phi}_p$ for ${\rm p} \neq 0$ in (A2.11). The complex envelope of the noisy slowly time-varying modulated signal becomes

$$\begin{aligned}\widetilde{V}(t) \cong V_0\sqrt{\frac{F_M}{2\Delta f}}&\left\{\sum_{n=-\frac{\Delta f_{\max}}{F_M}}^{n=\frac{\Delta f_{\max}}{F_M}} e^{j(n\omega_M t+\varphi_n)}\right.\\ &\times\left(1+\frac{\Delta\widetilde{V}_0+j\Delta\widetilde{\phi}_0}{2}e^{j\Omega t}\right.\\ &\left.\left.+\frac{\Delta\widetilde{V}_0^*+j\Delta\widetilde{\phi}_0^*}{2}e^{-j\Omega t}\right)\right\}.\end{aligned} \tag{A2.12}$$

APPENDIX III

Here, the relationship between complex envelopes of input and output signals in two-port circuit is discussed.

The relationship between $\widetilde{V}_{\rm in}(t)$ and $\widetilde{V}_{\rm out}(t)$ can be written as (17)

$$\widetilde{V}_{\rm out}(t) = \frac{1}{2}\left[H_+(\omega_o)\widetilde{V}_{\rm in}(t) - j\left.\frac{\partial H_+}{\partial\omega}\right|_{\omega_0}\frac{d\widetilde{V}_{\rm in}}{dt}\right]. \tag{A3.1}$$

The complex envelope of the input signal can be written as

$$\widetilde{V}_{\text{in}}(t) = \big(V_{o\_\text{in}} + \delta V_{\text{in}}(t)\big) e^{j(\Phi_{\text{in}}(t)+\delta\phi_{\text{in}}(t))}. \tag{A3.2}$$

The transfer function can be written

$$H_+(\omega) = \hat{H}_+(\omega) e^{j\psi(\omega)}. \tag{A3.3}$$

The partial derivative of $H_+(\omega)$ can be written as

$$\frac{\partial H_+}{\partial \omega} = H_+(\omega)\left[\frac{1}{\hat{H}_+}\frac{\partial \hat{H}_+}{\partial \omega} - j\tau_0\right] \tag{A3.4}$$

where $\tau_0 = -(\partial\Psi/\partial\omega)$ is the group delay of the linear circuit.

The time derivative of $\widetilde{V}_{\text{in}}(t)$ can be calculated from (A3.2) by a first-order expansion

$$\frac{d\widetilde{V}_{\text{in}}(t)}{dt} \approx \widetilde{V}_{\text{in}}(t)\left[\frac{1}{V_{o\_\text{in}}}\frac{d\delta V_{\text{in}}(t)}{dt} + j\left(\frac{d\delta\phi_{\text{in}}(t)}{dt} + \frac{d\Phi_{\text{in}}(t)}{dt}\right)\right]. \tag{A3.5}$$

By replacing (A3.5), (A3.4), (A3.3), and (A3.2) in (A3.1), we obtain

$$\begin{aligned}\widetilde{V}_{\text{out}}(t) \approx{}& \frac{1}{2}H_{o+}\widetilde{V}_{\text{in}}(t) \\ &\times\left\{1 - j\tau_0\left[\left(\frac{d\delta\phi_{\text{in}}(t)}{dt} + \frac{d\Phi_{\text{in}}(t)}{dt}\right) - j\frac{1}{V_{o\_\text{in}}}\frac{d\delta V_{\text{in}}(t)}{dt}\right]\right. \\ &\left. + \frac{1}{\hat{H}_{o+}}\left.\frac{\partial \hat{H}_+}{\partial\omega}\right|_{\omega_0}\left[\left(\frac{d\delta\phi_{\text{in}}(t)}{dt} + \frac{d\Phi_{\text{in}}(t)}{dt}\right)\right.\right. \\ &\left.\left. - j\frac{1}{V_{o\_\text{in}}}\frac{d\delta V_{\text{in}}(t)}{dt}\right]\right\}\end{aligned} \tag{A3.6}$$

where $H_{0+} = H_+(\omega_0)$ and $\hat{H}_{0+} = \hat{H}_+(\omega_0)$

As τ_0 is the circuit group delay, it is small compared to the envelop signal period, else we can develop at first order $\widetilde{V}_{\text{in}}(t-\tau_0)$ as follows:

$$\begin{aligned}\widetilde{V}_{\text{in}}(t-\tau_0) &\approx \widetilde{V}_{\text{in}}(t) - \tau_0\frac{d\widetilde{V}_{\text{in}}(t)}{dt} \\ &\approx \widetilde{V}_{\text{in}}(t)\times\left[1 - \tau_0\left(\frac{1}{V_{o\_\text{in}}}\frac{d\delta V_{\text{in}}(t)}{dt}\right.\right. \\ &\qquad\left.\left. + j\left(\frac{d\delta\phi_{\text{in}}(t)}{dt} + \frac{d\Phi_{\text{in}}(t)}{dt}\right)\right)\right].\end{aligned} \tag{A3.7}$$

By identifying with (A3.6), we obtain

$$\begin{aligned}\widetilde{V}_{\text{out}}(t) = \frac{1}{2}H_{o+}&\left\{\widetilde{V}_{\text{in}}(t-\tau_0) + \widetilde{V}_{\text{in}}(t)\right. \\ &\times\left[\frac{1}{\hat{H}_{o+}}\left.\frac{\partial\hat{H}_+}{\partial\omega}\right|_{\omega_0}\right. \\ &\times\left(\frac{d\delta\phi_{\text{in}}(t)}{dt} + \frac{d\Phi_{\text{in}}(t)}{dt}\right. \\ &\left.\left.\left. - j\frac{1}{V_{o\_\text{in}}}\frac{d\delta V_{\text{in}}(t)}{dt}\right)\right]\right\}.\end{aligned} \tag{A3.8}$$

The last approximation to consider is that $\omega\tau_0 \ll 1$, where ω is a low frequency of the envelop signal system that we can then write as

$$\begin{aligned}\widetilde{V}_{\text{out}}(t) = \frac{1}{2}H_{o+}&+\widetilde{V}_{\text{in}}(t) \\ &\times\left\{1 + \frac{1}{\hat{H}_{o+}}\left.\frac{\partial\hat{H}_+}{\partial\omega}\right|_{\omega_0}\right. \\ &\times\left(\frac{d\delta\phi_{\text{in}}(t)}{dt} + \frac{d\Phi_{\text{in}}(t)}{dt}\right. \\ &\left.\left. - j\frac{1}{V_{o\_\text{in}}}\frac{d\delta V_{\text{in}}(t)}{dt}\right)\right\}.\end{aligned} \tag{A3.9}$$

REFERENCES

[1] M. Camiade *et al.*, "Fully MMIC-based front end for FMCW automotive radar at 77 GHz," in *EUMC 2000*, vol. 1, Paris, France, pp. 9–12.

[2] M. Cartsen Metz *et al.*, "Fully integrated automotive radar sensor with versatile resolution," in *IEEE MTT-S Int. Microwave Symp. Dig.*, AZ, May 2001, pp. 1115–1118.

[3] M. Russell *et al.*, "Millimeter-wave radar sensor for automotive intelligent cruise control (ICC)," *IEEE Trans. Microwave Theory Tech.*, vol. 45, pp. 2444–2453, Dec. 1997.

[4] P. Bolcato *et al.*, "A unified approach of PM noise calculation in large RF multitone autonomous circuit," in *IEEE MTT-S Int. Microwave Symp. Dig.*, Boston, MA, June 2000, pp. 417–420.

[5] A. Laloue *et al.*, "New system-level simulation of noise spectra distortion in FM-CW autonomous cruise control radar," in *IEEE MTT-S Int. Microwave Symp. Dig.*, AZ, June 2002, pp. 459–462.

[6] S. O. Rice, "Envelopes of narrow-band signals," *Proc. IEEE*, vol. 70, pp. 692–699, July 1982.

[7] M. Lewis, "PLL's upconvert chirp radar signals," *Microwaves*, June 1981.

[8] M. Lax, "Classical noise: V noise in self sustained oscillators," *Phys. Rev.*, vol. 160, no. 2, pp. 290–307, Aug. 10, 1967.

[9] R. L. Kuvas, "Noise in single frequency oscillators and amplifiers," *IEEE Trans. Microwave Theory Tech.*, vol. MTT-21, pp. 127–134, Mar. 1973.

[10] K. Kurokawa, "Noise in synchronized oscillators," *IEEE Trans. Microwave Theory Tech.*, vol. MTT-16, pp. 234–240, Apr. 1968.

[11] A. Laloue *et al.*, "A measurement based model of HEMT taking into account the nonlinear, nonuniform, transmission line nature of the channel and its associated low frequency noise sources," in *GaAs Symp.*, Paris, France, Oct. 2000, pp. 181–185.

[12] ——, "A measurement based distributed low frequency noise HEMT model: Application to design of millimeter wave automotive radar chipset," in *IEEE MTT-S Int. Microwave Symp. Dig.*, AZ, May 2001, pp. 423–426.

Alban Laloue received the Ph.D. degree in electronics from the Universite de Limoges, Brive, France, in 2001.

He was initially involved in MMIC design with Alcatel Space Industries. Since the end of 2002, he has been a member of the engineer team with AMP-C3C, Les Ulis, France. He is currently involved with active antennas and the development of microwave phase shifters. His main research interest are transistor noise modeling and oscillator circuit simulation.

Jean-Christophe Nallatamby received the D.E.A. degree in microwave and optical communications and Ph.D. degree in electronics from the Universite de Limoges, Brive, France, in 1988 and 1992, respectively.

He is currently a Lecturer with the Department of Génie Electrique et Informatique Industrielle, Universite de Limoges. His research interests are nonlinear noise analysis of nonlinear microwave circuits, the design of the low phase noise oscillators, and the noise characterization of microwave devices.

Michel Prigent (M'93) received the Ph.D. degree from the Universite de Limoges, Brive, France, in 1987.

He is currently a Professor with the Universite de Limoges. His field of interest are the design of microwave and millimeter-wave oscillator circuits. He is also involved in characterization and modeling of nonlinear active components (FETs, pHEMTs, HBTs, etc.) with a particular emphasis on low-frequency noise measurement and modeling for the use in MMIC computer-aided design (CAD).

Marc Camiade was born in France, in 1958. He received the Dpl.Eng. degree in physics and electronic engineering from the Institut National des Sciences Appliquées, Toulouse, France, in 1981.

In 1982, he joined Thomson-CSF as a Design Engineer of hybrid circuits, during which time he participated in a variety of microwave and millimeter-wave circuits. Since 1988, he has been an Application Group Manager in charge of new product development based on microwave integrated circuit (MIC) and MMIC components. In 1996, he joined United Monolithic Semiconductors, Orsay, France, where he is currently in charge of the development of components for defense and automotive applications. He is also currently and mainly involved in all the functions for radar front-ends from L- to W-bands.

Juan Obregon (SM'91) received the E.E. degree from the Conservatoire National des Arts et Métiers (CNAM), Paris, France, in 1967, and the Ph.D. degree from the Universite de Limoges, Brive, France, in 1980.

He then joined the Radar Division, Thomson-CSF, where he contributed to the development of parametric amplifiers for radar front-ends. He then joined RTC Laboratories, where he performed experimental and theoretical research on Gunn oscillators. In 1970, he joined the DMH Division, Thomson-CSF, and became a Research Team Manager. In 1981, he was appointed Professor at the Universite de Limoges. He is currently Professor Emeritus with the Universite de Limoges. Since 1981, he has been a consultant to microwave industrial laboratories. His fields of interest are the modeling, analysis, and optimization of nonlinear microwave circuits, including noise analysis.